Sofiane MENDACI[1], Mohamed Rachid MEKIDECHE[2], Ali REZIG[2]

University of Guelma (1), University of Jijel (2), Algeria

Analytical Calculation of Magnetic Field in Surface-Mounted Permanent Magnet Motors Taking Into Account Slotting Effect

***Abstract**. This paper presents an analytical approach to calculate the magnetic field distribution in surface-mounted permanent magnet motors. The technique is based on 2D solution of the Maxwell's equations using the separation of variable method. The magnetic field expressions are developed in slots regions, magnetic air gap region and permanent magnet region leading to an exact calculation of the slot effects on the air gap magnetic quantities. Magnetic field and cogging torque computed with the proposed analytical method are validated through finite-element analysis.*

***Streszczenie.** W artykule zaprezentowano analityczną metodę obliczania rozkładu pola magnetycznego w powierzchniowo montowanym silniku z magnesami trwałymi. Pola magnetyczne było liczone w przestrzeni między szczelinami oraz rejonie nabiegunników. (**Analityczne wyznaczane rozkładu pola magnetycznego w silniku z magnesami trwałymi montowanym powierzchniowo z uwzględnieniem efektu szczelin**)*

Keywords: Analytical calculation, finite element method, surface mounted permanent magnet motors, magnetic field.
Słowa kluczowe: obliczanie pola magnetycznego, metoda element skończonego, silnik.

Introduction

In the last few years the manufacturers of electrical machines have shown a growing interest for permanent magnet brushless machines (PMBMs). This interest is mainly due to the high efficiency, high reliability, high power density, high power factor, small size and decreasing cost of magnets. Different topologies of PM machines are available e.g. radial flux machines, axial flux machines and transversal flux machines [1, 2]. The accurate knowledge of the magnetic field distribution in the air gap is prerequisite for predicting PMBM performance such as electromagnetic torque, back electromotive (EMF), stator losses, demagnetization limit, winding inductances, eddy current losses in the rotating parts, noise and vibration, etc.[3]. Numerical methods of field analysis such as finite elements or boundary integral methods provide accurate results considering geometric details and nonlinearity of magnetic materials but they are computer time consuming and does not easily allow a parametric study in a design procedure. However, they are not explicit compared to the analytical methods [4].

In analytical modelling of electrical machines, one of the most difficult tasks is to take into account the slotting effect in air gap magnetic field prediction. The presence of stator/rotor slots have a large influence on the air gap magnetic field distribution and therefore on the electromagnetic torque. The consequences can be torque ripples causing vibration, noise and speed fluctuations. Many analytical field methods exist in the literature, most of them do not take into account saturation and slotting effect in an explicit manner [4, 5, 6, 7].

This paper attempts to provide analytical tools to facilitate the analysis and design of surface-mounted permanent magnet brushless machines with taking into account stator slotting in an explicit manner. The developed model, in this paper, embraces both internal and external topologies. The magnetic field distribution is established by analytically solving Maxwell's equations in the different sub-domains (magnet, air gap and stator slots) of the machine, thanks to separation of variables method.

The paper is organized as follows. First, the problem description and the assumption of the model are presented in section II. The analytical method for magnetic field calculation in the different sub-domains is then described. Finally, the analytical results are verified with finite-element method.

Problem description and assumptions

The general configuration of a surface-mounted permanent magnet motor considered in the present work is shown in Fig. 1.

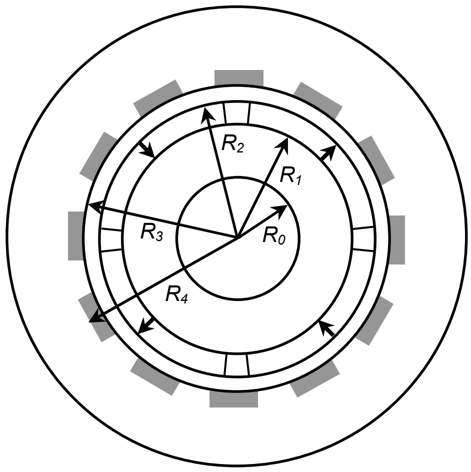

Fig.1. Surface-mounted permanent magnet motor

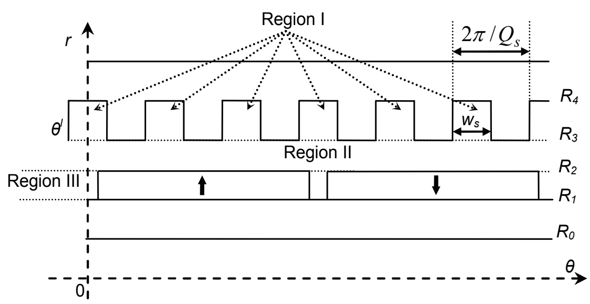

Fig.2. Idealized machine model

The analytical method used in this paper is based on analysis of 2-D model in polar coordinates. The analytical solution for the field distribution is set to cover only low permeability regions (slot (region I), air gap (region II), and permanent magnet (region III) regions) and is established based on the following assumptions [7]:

1. The stator and rotor cores are assumed to be infinitely permeable.
2. Permanent magnets have a linear demagnetization characteristic.
3. End effect and saturation are neglected.
4. Eddy current effects are neglected (no eddy current loss in the magnets or armature windings).

Magnetic field distribution produced by magnets

Fig. 2 shows the series-slot model with a pole-pair pitch of the idealized permanent magnet machine with principal dimensions and different field regions. In various regions, the flux density $\boldsymbol{B}$ and field intensity $\boldsymbol{H}$ are expressed as:

(1) $\boldsymbol{B} = \mu_0 \boldsymbol{H}$ In regions I and II

(2) $\boldsymbol{B} = \mu_0 \mu_r \boldsymbol{H} + \mu_0 \boldsymbol{M}$ In region III

where μ_r is the relative recoil permeability, $\boldsymbol{M}$ is the magnetization vector of permanent magnets. The direction of $\boldsymbol{M}$ depends on the orientation and magnetization of permanent magnets. In polar coordinates, the magnetization vector $\boldsymbol{M}$ is expressed as:

(3) $\boldsymbol{M} = M_r \boldsymbol{e}_r + M_\theta \boldsymbol{e}_\theta$

and remanent magnetization vector $\boldsymbol{M}$ components can be expressed by Fourier series as follows:

(4) $$\begin{cases} M_r = \sum_{k=1}^{\infty} \left(M_{r1k} \cos(kp\theta) + M_{r2k} \sin(kp\theta) \right) \\ M_\theta = \sum_{k=1}^{\infty} \left(M_{\theta 1k} \cos(kp\theta) + M_{\theta 2k} \sin(kp\theta) \right) \end{cases}$$

p is the pole pair number.

By using the Maxwell's equations, the partial differential equation for quasi-stationary magnetic fields created only by permanent magnets in a continuous and isotropic region can be expressed in terms of the magnetic vector potential $\boldsymbol{A}$ by:

(5) $\nabla^2 \boldsymbol{A} = 0$ In region I and II

(6) $\nabla^2 \boldsymbol{A} = -\mu_0 \nabla \times \boldsymbol{M}$ In region III

$\boldsymbol{A}$ only has A_z component which is independent of z (infinitely long machine in axial direction).

In polar coordinates, the equations (5) and(6) can be rewritten as:

(7) $$\frac{\partial^2 A_z}{\partial r^2} + \frac{1}{r}\frac{\partial A_z}{\partial r} + \frac{1}{r^2}\frac{\partial^2 A_z}{\partial \theta^2} = \begin{cases} 0 & \text{In region I and II} \\ -\mu_0 \nabla \times \boldsymbol{M} & \text{In region III} \end{cases}$$

By using the method of separating variables and the superposition law, the general solution of (7) can be written as:

(8) $$A_z = a_0 + A_{ps} + \sum_{k=1}^{\infty} \begin{pmatrix} \left(c_{1k} r^{kp} + c_{2k} r^{-kp} \right) \cos(kp\theta) \\ + \left(c_{3k} r^{kp} + c_{4k} r^{-kp} \right) \sin(kp\theta) \end{pmatrix}$$

where A_{ps} is the particular solution of the equation (7) for only the permanent magnets region (region III), given by:

(9) $$A_{ps} = r \sum_{k=1}^{\infty} \left(A_{1k} \cos(kp\theta) + A_{2k} \sin(kp\theta) \right)$$

Coefficients A_{1k} and A_{2k} are given by:

(10) $$\begin{cases} A_{1k} = \mu_0 \dfrac{kpM_{r2k} - M_{\theta 1k}}{1 - (kp)^2} \\ \\ A_{2k} = -\mu_0 \dfrac{kpM_{r1k} + M_{\theta 2k}}{1 - (kp)^2} \end{cases} \quad \text{if } kp \neq 1$$

and

(11) $$\begin{cases} A_{1k} = \dfrac{\mu_0}{2} \left(M_{r2k} - M_{\theta 1k} \right) \ln(r) \\ \\ A_{2k} = -\dfrac{\mu_0}{2} \left(M_{r1k} + M_{\theta 2k} \right) \ln(r) \end{cases} \quad \text{if } kp = 1$$

The radial and tangential components of the flux density are deduced from A_z by:

(12) $$B_r = \frac{1}{r}\frac{\partial A_z}{\partial \theta} \quad \text{and} \quad B_\theta = -\frac{\partial A_z}{\partial r}$$

a) Stator slots (region I)

The slotted stator is assumed to have Q_s slots which are numbered $l=0,...,Q_s-1$. In the slot l, the no-load magnetic field satisfies the following boundary conditions:

(13) $$\begin{cases} B_\theta^I (R_4, \theta) = 0 \\ B_r^I \left(r, \theta^l \right) = 0 \text{ and } B_r^I \left(r, \theta^l + w_s \right) = 0 \end{cases}$$

where: $\theta^l = l \dfrac{2\pi}{Q_s} - \dfrac{w_s}{2}$

With these boundary conditions, the general expressions of the flux density components in the slots area l are given by:

(14) $$B_r^I = -\sum_{m=1}^{\infty} \left(\frac{m\pi}{w_s r} f_m^l G_m(r) \sin\left(\frac{m\pi}{w_s} \left(\theta - \theta^l \right) \right) \right)$$

(15) $$B_\theta^I = -\sum_{m=1}^{\infty} \left(f_m^l \frac{\partial G_m(r)}{\partial r} \cos\left(\frac{m\pi}{w_s} \left(\theta - \theta^l \right) \right) \right)$$

where:

$$G_m(r) = \left(\frac{r}{R_4} \right)^{\frac{m\pi}{w_s}} + \left(\frac{r}{R_4} \right)^{-\frac{m\pi}{w_s}}$$

b) Air gap (region II)

The general solution of the flux density components in this region is:

(16) $$B_r^{II} = -\sum_{k=1}^{\infty} \frac{pk}{r} \begin{pmatrix} \left(c_{1k}^{II} r^{kp} + c_{2k}^{II} r^{-kp} \right) \sin(kp\theta) \\ - \left(c_{3k}^{II} r^{kp} + c_{4k}^{II} r^{-kp} \right) \cos(kp\theta) \end{pmatrix}$$

$$(17)\quad B_{\theta}^{II} = -\sum_{k=1}^{\infty}\frac{pk}{r}\begin{pmatrix}\left(c_{1k}^{II}r^{kp}-c_{2k}^{II}r^{-kp}\right)cos\left(kp\theta\right)\\ +\left(c_{3k}^{II}r^{kp}-c_{4k}^{II}r^{-kp}\right)sin\left(kp\theta\right)\end{pmatrix}$$

The continuity condition between the region I (stator slots) and the region II (air gap) leads to:

$$(18)\quad \begin{cases}B_{\theta}^{II}\left(R_3,\theta\right)=B_{\theta}^{I}\left(R_3,\theta\right) \\ \qquad\qquad\qquad \text{for } \theta\in\left[\theta^{l};\theta^{l}+w_s\right] \\ B_{r}^{II}\left(R_3,\theta\right)=B_{r}^{I}\left(R_3,\theta\right)\end{cases}$$

and between region II and stator tooth adjacent to slots is given by:

$$(19)\quad B_{\theta}^{II}\left(R_3,\theta\right)=0 \quad \text{for} \quad \theta\in\left[\theta^{l}+w_s;\theta^{l+1}\right]$$

The treatment of the interface conditions (18) and (19) yields to the following relations between Fourier series coefficients of region II.

$$(20)\quad \begin{cases}pk\left(c_{2k}^{II}R_3^{-kp}-c_{1k}^{II}R_3^{kp}\right)= \\ \quad\sum_{n=1}^{\infty}pn\left(h\left(k,n\right)-f\left(k,n\right)\right)\left(c_{1n}^{II}R_3^{np}+c_{2n}^{II}R_3^{-np}\right) \\ pk\left(c_{4k}^{II}R_3^{-kp}-c_{3k}^{II}R_3^{kp}\right)= \\ \quad\sum_{n=1}^{\infty}pn\left(h\left(k,n\right)+f\left(k,n\right)\right)\left(c_{3n}^{II}R_3^{np}+c_{4n}^{II}R_3^{-np}\right)\end{cases}$$

where:

$$f\left(k,n\right)=\begin{cases}\frac{w_sQ_s}{2\pi}\sum_{m=1}^{\infty}\left(\frac{\left(\frac{\partial G_m}{\partial r}\right)\left(R_3\right)}{G_m\left(R_3\right)}L_1\right) & \text{if}\left(k+n\right)=q\frac{Q_s}{p} \\ 0 & \text{if}\left(k+n\right)\neq q\frac{Q_s}{p}\end{cases}$$

and

$$h\left(k,n\right)=\begin{cases}\frac{w_sQ_s}{2\pi}\sum_{m=1}^{\infty}\left(\frac{\left(\frac{\partial G_m}{\partial r}\right)\left(R_3\right)}{G_m\left(R_3\right)}L_2\right) & \text{if}\left(k-n\right)=q\frac{Q_s}{p} \\ 0 & \text{if}\left(k-n\right)\neq q\frac{Q_s}{p}\end{cases}$$

L_1 and L_2 are given by:

$$L_1=L\left(cos\left(p\left(n+k\right)\frac{w_s}{2}\right)-\left(-1\right)^m cos\left(p\left(n-k\right)\frac{w_s}{2}\right)\right)$$

$$L_2=L\left(cos\left(p\left(n-k\right)\frac{w_s}{2}\right)-\left(-1\right)^m cos\left(p\left(n+k\right)\frac{w_s}{2}\right)\right)$$

$$\text{with:}\quad L=\begin{pmatrix}\left(\frac{1}{m\pi+kpw_s}-\frac{1}{m\pi-kpw_s}\right) \\ \times\left(\frac{1}{m\pi+npw_s}-\frac{1}{m\pi-npw_s}\right)\end{pmatrix}$$

c) Permanent magnets (region III)

The boundary condition for this region is:

$$(21)\quad B_{\theta}^{III}\left(R_2,\theta\right)=\mu_0 M_{\theta}$$

In the present work, the remanence of permanent magnet is considered to be ideal and oriented in the radial direction yielding to: M_{θ}=0.

The general expressions of the flux density components subject to boundary condition (21) are given by:

$$(22)\quad B_r^{III}=\begin{cases}\sum_{k=1}^{\infty}kp\left(A_{2k}\,cos\left(kp\theta\right)-A_{1k}\,sin\left(kp\theta\right)\right) \\ +\sum_{k=1}^{\infty}\frac{pk}{r}\begin{pmatrix}c_{3k}^{III}\left(r^{kp}+R_1^{2kp}r^{-kp}\right)cos\left(kp\theta\right) \\ -c_{1k}^{III}\left(r^{kp}+R_1^{2kp}r^{-kp}\right)sin\left(kp\theta\right)\end{pmatrix}\end{cases}$$

$$(23)\quad B_{\theta}^{III}=-\left\{\sum_{k=1}^{\infty}\frac{pk}{r}\begin{pmatrix}c_{1k}^{III}\left(r^{kp}-R_1^{2kp}r^{-kp}\right)cos\left(kp\theta\right) \\ -c_{3k}^{III}\left(r^{kp}-R_1^{2kp}r^{-kp}\right)sin\left(kp\theta\right)\end{pmatrix}\right.$$

The continuity condition between the region II (air gap) and the region III (PMs) are given by:

$$(24)\quad B_r^{II}\left(R_2,\theta\right)=B_r^{III}\left(R_2,\theta\right)\;;\;B_{\theta}^{II}\left(R_2,\theta\right)=B_{\theta}^{III}\left(R_2,\theta\right)$$

The exploitation of this interface conditions yields to the following relations between coefficients of regions II and III.

(25)

$$\begin{cases}c_{1k}^{II}=c_{1k}^{III}+\frac{R_2^{-kp+1}}{2}A_{1k} \text{ and } c_{2k}^{II}=c_{1k}^{III}R_1^{2kp}+\frac{R_2^{kp+1}}{2}A_{1k} \\ c_{3k}^{II}=c_{3k}^{III}+\frac{R_2^{-kp+1}}{2}A_{2k} \text{ and } c_{4k}^{II}=c_{3k}^{III}R_1^{2kp}+\frac{R_2^{kp+1}}{2}A_{2k}\end{cases}$$

Combining (20) and (25) yields:

(26)

$$\begin{pmatrix}-k\left(R_3^{kp}-R_3^{-kp}R_1^{2kp}\right)c_{1k}^{III}- \\ \sum_{n=1}^{\infty}n\left(R_3^{np}+R_3^{-np}R_1^{2np}\right)\left(h\left(k,n\right)-f\left(k,n\right)\right)c_{1n}^{III}\end{pmatrix}=$$

$$\begin{pmatrix}\frac{k}{2}\left(R_3^{kp}R_2^{-kp+1}-R_3^{-kp}R_2^{kp+1}\right)A_{1k}+ \\ \sum_{n=1}^{\infty}\frac{n}{2}\left(R_3^{np}R_2^{-np+1}+R_3^{-np}R_2^{np+1}\right)\left(h\left(k,n\right)-f\left(k,n\right)\right)A_{1n}\end{pmatrix}$$

(27)

$$\begin{pmatrix}-k\left(R_3^{kp}-R_3^{-kp}R_1^{2kp}\right)c_{3k}^{III}- \\ \sum_{n=1}^{\infty}n\left(R_3^{np}+R_3^{-np}R_1^{2np}\right)\left(h\left(k,n\right)+f\left(k,n\right)\right)c_{3n}^{III}\end{pmatrix}=$$

$$\begin{pmatrix}\frac{k}{2}\left(R_3^{kp}R_2^{-kp+1}-R_3^{-kp}R_2^{kp+1}\right)A_{2k}+ \\ \sum_{n=1}^{\infty}\frac{n}{2}\left(R_3^{np}R_2^{-np+1}+R_3^{-np}R_2^{np+1}\right)\left(h\left(k,n\right)+f\left(k,n\right)\right)A_{2n}\end{pmatrix}$$

The resolution of the above systems (26) and (27) by an iterative method gives the Fourier series coefficients (c_{1k}^{III} and c_{3k}^{III}) of the magnetic field in the permanent magnet region and the air gap magnetic field coefficients are deduced by means of (25). Hence, the magnetic field is completely defined in all regions.

Cogging torque computation

The torque developed on the motor can be obtained by calculating the Maxwell stress tensors method in the air gap [4].

$$T_{cog} = \frac{LR_2^2}{\mu_0} \int_0^{2\pi} B_r^{II} B_\theta^{II} \, d\theta \qquad (28)$$

Incorporating (16) and (17) in (28) and integrating, the final expression of the cogging torque is given by:

$$T_{cog} = \frac{L 2\pi}{\mu_0} \sum_{k=1}^{\infty} (kp)^2 \left(c_{2k}^{II} c_{3k}^{II} - c_{1k}^{II} c_{4k}^{II} \right) \qquad (29)$$

where L is the effective axial length.

Calculation results

In order to asses the validity of the proposed analytical method, the corresponding results obtained by finite element method (FEM) are provided for comparison. The specifications of the motor are listed in Table 1.

Table 1. The parameters of the PM motor

Symbol	Quantity	Value
p	Number of pole pairs	2
Q_s	Number of stator slots	12
R_1	Radius of the rotor yoke surface	69 [mm]
R_2	Radius of the PM surface	79 [mm]
R_3	Inner radius of the stator	82 [mm]
R_4	Radius of the stator yoke surface	92 mm]
L	Axial length	40 [mm]
B_r	Magnet remanent flux density	0.8 [T]
w_s	Slot opening	14 [Degree]
α_p	Magnet-arc to pole-pitch ratio	0.933

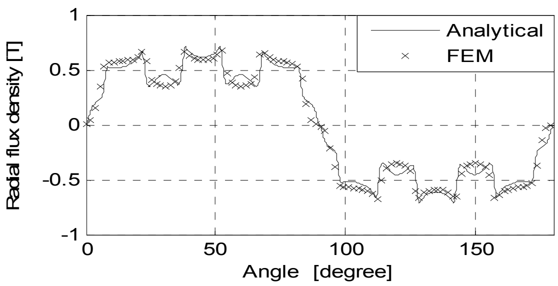

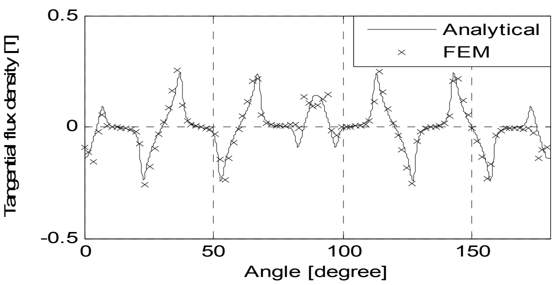

Fig.3. Waveforms of the radial and tangential flux density in the middle of the air gap region (r= (R_3 + R_2)/2)

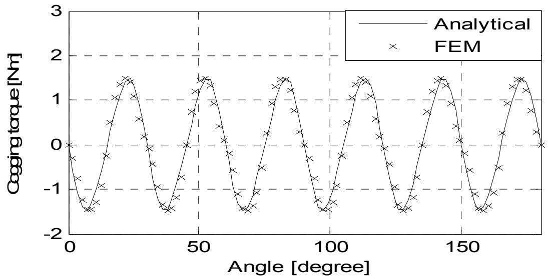

Fig.4. Cogging torque waveform

Fig. 3 compares analytically predicted and finite element calculated open-circuit distributions of magnetic flux density components in the air gap region. It can be seen that the analytical results agree well with the FEM results.

Fig. 4 compares cogging torque waveforms obtained by both techniques (Analytical and FEM). Again, the results are in good agreement.

Conclusion

In this paper an accurate analytical approach to calculate the magnetic field distribution in surface-mounted permanent magnet motor considering slotting effects has been presented and verified. By calculating the Maxwell stress tensor in the air gap, the cogging torque can be deduced. The anytical results are in good agreement with that obtained by finite element method, which enables the proposed analytical approach to be a useful tool for analysis, design and optimization of surface-mounted PM slotted motors

REFERENCES

[1] Chau K. T., Chan C. C., Liu C., Overview of Permanent Magnet Brushless Drives for Electric and Hybrid Electric Vehicles, *IEEE Trans Ind. Electr.*, 55 (2008), No. 6, 2246-2257

[2] Mi C. C., Analytical Design of Permanent Magnet Traction Drive Motors, *IEEE Trans. Magn.*, 42 (2006), No. 7, 1861-1866

[3] Li Zhu, S. Z. Jiang, Z. Q. Zhu, C. C. Chan, Analytical Methods for Minimizing Cogging Torque in Permanent-Magnet Machines, *IEEE Trans. Magn.*, 45 (2009), No. 6, 2023-2031

[4] Z. Q. Zhu, L. J. Wu, Z. P. Xia, An Accurate Subdomain Model for Magnetic Field Computation in Slotted Surface-Mounted Permanent-Magnet Machines, *IEEE Trans. Magn.*, 46 (2010), No. 4, 1100-1115

[5] A. Rezig, M. R. Mekideche, A. Djedir, Impact of Rotor Eccentricity faults on Noise Generation in Permanent Magnet Synchronous Motors, *Przegląd Elektrotechniczny*, 39 (2011), nr 1, 189-194

[6] Z. Q. Zhu, D. Howe, C. C. Chan, Improved Analytical Model for Predicting the Magnetic Field Distribution in Brushless Permanent-Magnet Machines, *IEEE Trans. Magn.*, 38 (2002), No. 1, 229-238

[7] T. Lubin, S. Mezani, A. Rezzoug, Exact Analytical Model for Magnetic Field Computation in the AirGap of Cylindrical Machines Considering Slotting Effects, *IEEE Trans. Magn.*, 46 (2010), No. 4, 1092-1099

***Authors**: Dr. Sofiane Mendaci, University of Guelma, Department of Electrical Engineering, BP 401, 24000, Algeria, E-mail: smendaci2000@yahoo.fr; Pro. dr. Mohamed Rachid Mekideche, University of Jijel, LAMEL, BP 98 Ouled Aissa, 18000, Algeria, E-mail: mek_moh@yahoo.fr, Dr. Ali Rezig, University of Jijel, LAMEL, BP 98 Ouled Aissa, 18000, Algeria, E-mail: alirezikdz@yahoo.fr*